ACS ES&T Water

pubs.acs.org/estwater

Review

Carbon Nanopore-Tailored Reverse Osmotic Water Desalination

Yuchen Liu, Zimeng Zhang, and Shiren Wang*

Cite This: https://dx.doi.org/10.1021/acsestwater.0c00015

Read Online

ACCESS | Metrics & More | Article Recommendations

ABSTRACT: Water desalination is receiving an increasing amount of attention because of the global concern of sustainability. Emerging nanoporous materials are investigated to selectively separate ions for producing freshwater. This review addresses the role of nanopores in ion/water separation and then discusses current efforts and state-of-the-art methods regarding the effect of nanopore geometry on the water desalination process and performance, particularly carbon nanostructure-based water desalination. Finally, the prospect of nanopore-induced water desalination is described.

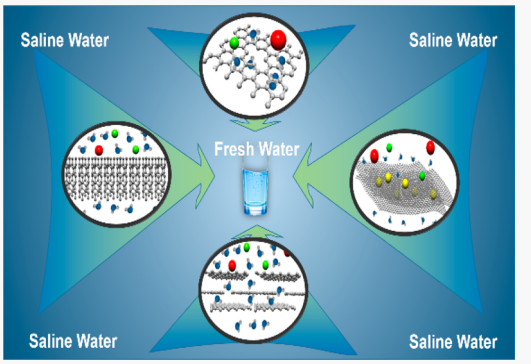

1. INTRODUCTION

Water resources are irreplaceable and fundamental elements whose usage has increased worldwide by 1% per year since the 1980s,[1] but at present, humans are suffering from a severe freshwater crisis that is compromising food security and public health.[2] The rising demand for freshwater makes the situation even worse due to the rapid population growth of the global population, urbanization, rapid industrialization, global climate change, and more stringent health-based water quality standards.[3] Global water demand is expected to increase by 20−30% between now and 2050. Although 71% of the earth's surface is covered by water, more than 96% of this water is held by the oceans as saline water. The remaining freshwater also includes glaciers, ice caps, groundwater, and surface water, which means only <1% of the water on the Earth is readily usable for domestic activities and agriculture.[4] Unfortunately, the distribution of freshwater resources on the earth is seriously uneven. According to a satellite-based study, the dry areas of the earth are becoming drier while the wet areas are becoming wetter, which intensifies the current severe situation.[5]

Generally, water can be classified into the following levels on the basis of the concentration of dissolved solids in milligrams per liter (ppm) as seawater (>10000 ppm), brackish water (1000−10000 ppm), and freshwater (<1000 ppm). Freshwater is the common water resource for daily life and the development of society. As the demand for freshwater increases, unconventional water sources such as stormwater, brackish water, industrial wastewater, and seawater are being considered for use, especially in some water-stressed areas. Seawater is the most inexhaustible water source on the earth, but its high salinity constrains its application in domestic activities. Brackish water, which comes from brackish fossil aquifers and is a byproduct of human activity and the waste product of the salinity gradient power process, is common the world over. Texas, for example, has abundant underground water, including 880 trillion gallons of primarily brackish groundwater. In this case, the desalination process is one of the best strategies for acquiring freshwater from saline water to meet the increasing demand. Desalination is defined as the process that removes salts and other dissolved solids from either seawater or brackish water to yield freshwater suitable for human consumption and industrial and domestic requirements.[6] Generally, desalination methods can be classified as distillation (including multistage flash distillation and multiple-effect distillation), ion exchange, membrane processes, freezing desalination, geothermal desalination, electrodeionization (EDI), and solar desalination.[7] The membrane processes that are driven by hydraulic pressure can be distinguished as reverse osmosis/forward osmosis (RO/FO), nanofiltration (NF), ultrafiltration (UF), and microfiltration (MF) on the basis of the feature size (as shown in Figure 1A).

The main function of MF and UF membranes is to retain suspended particles and macromolecules. The mass transport in MF and UF membranes is governed by a size or sieving exclusion mechanism. On the contrary, NF and RO focus on removing nearly all kinds of ions to reduce water salinity. The

Received: June 6, 2020
Revised: July 23, 2020
Accepted: August 3, 2020

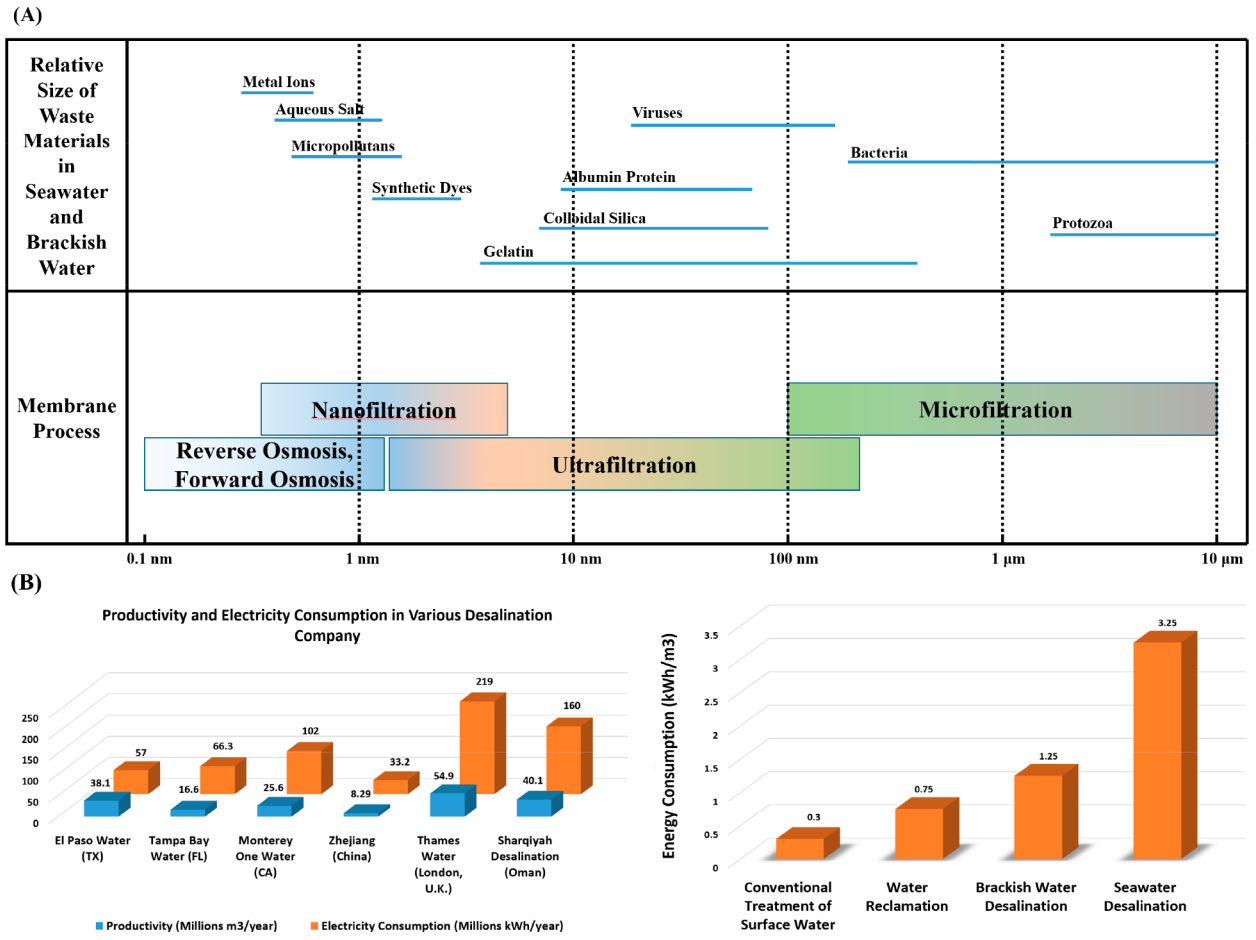

Figure 1. (A) Membrane processes for water purification and the corresponding size of waste materials in seawater and brackish water. (B) Energy consumption of industrial RO desalination plants and other water treatments.

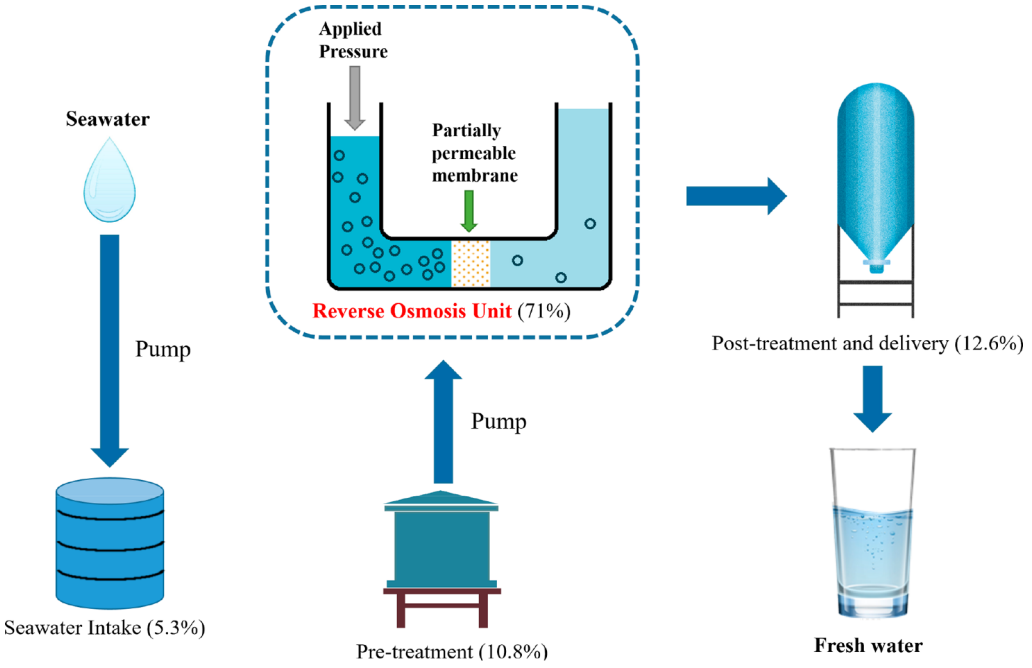

Figure 2. Process diagram of a seawater RO desalination plant with the energy consumption ratio of each step.

molecular separation of RO is based on the solution−diffusion mechanism. The separation mechanism of NF is a combination of sieving exclusion and solution−diffusion. Specifically, >65% of the installed desalination capacity is based on the RO

https://dx.doi.org/10.1021/acsestwater.0c00015
ACS EST Water XXXX, XXX, XXX−XXX

desalination process.[8] RO desalination is a water purification technology that uses applied pressure to overcome the osmotic pressure to separate the water molecule from the saline solution with the help of a partially permeable membrane. Compared with thermal distillation as well as other desalination methods, RO technology has great advantages in being a continuous process, mild working conditions, energy efficiency, a low level of environmental pollution, and being facile.[9] However, the conflict between desalination efficiency and the consumption of a huge amount of energy is still the biggest obstacle to the further development of desalination technologies. Figure 1B compares the productivity and electricity consumption in various desalination companies the world over as well as the energy consumption of different water treatment methods. As shown in the figure, the energy consumption for seawater purification is 10 times larger than that of surface water treatment.

In a RO desalination plant, seawater is subjected to extraction, pretreatment, reverse osmosis treatment, post-treatment, and finally storage as drinking water (as shown in Figure 2). In a typical seawater desalination plant using Pacific Ocean water that has a level of total dissolved solids (TDS) of 33.5 g/L, the overall energy consumption is 3.57 kWh/m^3 and the RO unit accounts for 71% of total energy consumption.[10] In the RO unit, membranes are the most essential components that directly determine water purification performance. A high-quality RO membrane should possess high water permeability, high ion selectivity, long-term stability, antifouling properties, and good scalability. Currently, commercial RO membranes are mainly polyamide (PA) thin composite film (TFC) and its derivatives, which have drawbacks such as their low water permeability, high energy consumption, strong fouling tendency, and limited lifetime.[11] Therefore, the research goals for membrane technologies for RO desalination are to reduce energy consumption, to improve desalination performance especially focusing on the water flux, and to improve antifouling performance. In particular, there is still much progress to be made for current lab-made membranes to meet industrial production needs.

To overcome these obstacles, the new generation of RO membranes introduces nanomaterials. Nanomaterials, which are in the range of <100 nm, such as zeolites, metal−organic frameworks, ceramics, carbon-based materials, and aquaporin (AQP) have attracted considerable attention as alternative membrane materials due to their good chemical resistance, high flux, and high rejection rate.[12−17] Although these materials are promising, their practical performance has not yet been fully demonstrated. Membranes consisting of zeolites and ceramics are difficult to shape in a cost-effective manner. Other two-dimensional (2D) materials such as WS_2[18] and MoS_2[19−21] also suffer from high material cost and scalability. Among all kinds of nanomaterials, carbon-based materials, such as carbon nanotubes (CNTs) and graphene, possess great potential in water desalination[11,15−17] and gas and ion sepration[22−26] because of unique properties such as their size- and shape-dependent properties, environmentally benign nature, abundance, and ease of handling.

Previously, many studies have reviewed the research on water desalination, which mainly classify the membranes by the materials used.[3,11,27−36] This classification method is straightforward for the researchers and makes it easy to follow the evolution of the research. However, it fails to summarize the influence of the pore geometric structure of RO membranes that is more critical to water desalination performance. On the contrary, several literature reviews have also focused on 2D materials.[35,37−39] This review will give an overview of the state-of-the-art desalination membrane using a different classification method based on the nanopore geometric structures. Their pore structure and corresponding manufacturability, including scalability, cost-effectiveness, and quality, will be compared. This review is the first to address relationships between pore structure and membrane performance, providing a refreshing view of next-generation RO membranes for water desalination.

2. MECHANISM OF THE DESALINATION PROCESS

For water desalination, the most significant conflict occurs between permeability and selectivity. In a common implication, an increase in permeability for a highly permeating species such as water molecules will lead to a larger increase in permeability for relatively strongly retained species such as salts.[40] As indicated before, the mass transport in MF and UF membranes is dominated by a size or sieving exclusion mechanism, the molecular separation of RO is based on the solution−diffusion mechanism, and the separation mechanism of NF is a combination of sieving exclusion and solution−diffusion. Herein, it is necessary to discuss the mechanism of the desalination process before investigating the performance of different membranes with respect to water desalination.

2.1. Porous Membrane. Generally, for both porous membranes (including MF and UF), water flux through membranes can be described by a hydrodynamic model:[41]

$$J_w = \left(\frac{K_w D_w V_w c_{w0}}{LRT}\right)(\Delta P - \Delta\pi) = A(\Delta P - \Delta\pi_m) \quad (1)$$

where J_w is the water flux, A is the water permeability coefficient, ΔP is the applied hydraulic pressure, $\Delta\pi_m$ is the osmotic pressure difference across the active membrane, K_w is a constant determined by the standard chemical potentials of water, D_w is the diffusion coefficient, c_{w0} is the initial concentration of water, V_w is the molar volume of water, R is the gas constant, T is the absolute temperature, and L is the thickness of the membrane.

Similarly, the salt flux can be modeled as Fickian diffusion as eq 2:[42]

$$J_s = \frac{D_s K_s}{L}\Delta c_s = B\Delta c_s \quad (2)$$

where J_s is the solute flux, B is the solute permeability coefficient, Δc_s is the solute concentration difference, K_s is a constant determined by the standard chemical potentials of the solute, and D_s is the diffusion coefficient of the solute. The performance of an RO membrane is determined by the terms A and B. In MF and UF membranes, $\Delta\pi_m$ is negligible, which means the water flux is proportional to the applied pressure, while in RO and NF membranes, $\Delta\pi_m$ is a critical parameter.

2.2. Nonporous Membranes. For nonporous membranes, the water flux also follows the hydrodynamic model, but the transportation of the water and solute is dominated by the solution−diffusion model. Both water and solute molecules move into the selective layer of the membrane, diffuse through the interlayer gap, and desorb on the permeate side. The combination of solubility and diffusivity defines the diffusive permeability of the water (P_w) and solute (P_s), which are intrinsic properties of the materials and independent of

https://dx.doi.org/10.1021/acsestwater.0c00015
ACS EST Water XXXX, XXX, XXX−XXX

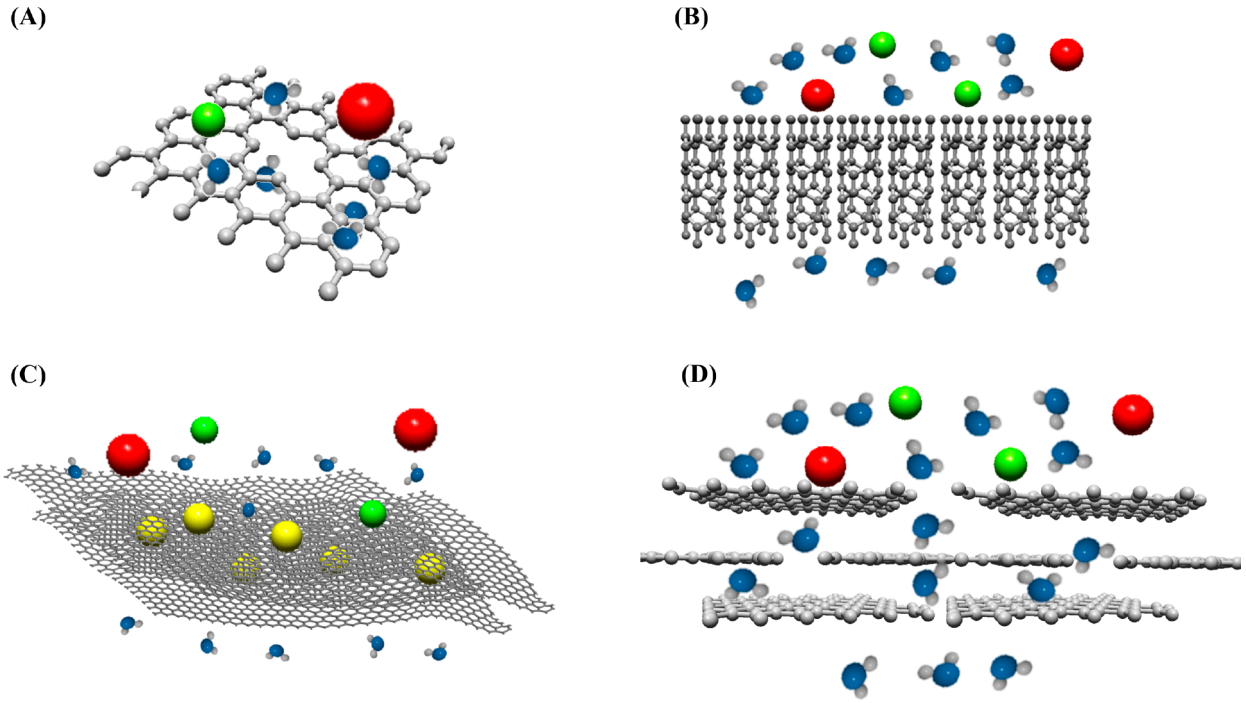

Figure 3. Schematic of the mechanism of water desalination for different pore geometric structures. The pore geometric structure can be classified as a porous structure, including (A) a horizontal pore on the active layer and (B) a hollow nanochannel, or as a nonporous structure, including (C) a tent-shaped lateral channel and (D) a quasi-uniform lateral channel.

membrane thickness. Therefore, A and B of nonporous membranes can be defined as

$$A_{np} = \frac{P_w V_w}{LRT} \tag{3}$$

$$B_{np} = \frac{P_s}{L} \tag{4}$$

For porous membranes, water flow through the active layer can be simplified as vertical flow through cylindrical holes. Therefore, the term A of porous membranes can be defined as

$$A_p = \frac{\varepsilon r_p^{\,2}}{8\mu L} \tag{5}$$

where μ is the solution viscosity, ε is the surface porosity, and r_p is the pore radius. From eq 5, r_p has a positive effect on water permeability. On the contrary, the pore structure determines the local pore radius of the nanopores, which is more accurate than the average pore size of the membrane. Hence, it is important to classify the RO membranes by their geometric structures. The solutes with the porous membranes can be fully rejected if the largest pore radius (r_p) is smaller than the radius of the solute (r_s). If $r_p \geq r_s$, then the rejection rate can be expressed as an empirical formula:[40]

$$R = 1 - \left[2\left(1 - \frac{r_s}{r_p}\right)^2 - \left(1 - \frac{r_s}{r_p}\right)^4\right] \exp\left[-0.7146\left(\frac{r_s}{r_p}\right)^2\right] \tag{6}$$

On the contrary, for a specific membrane, water permeability A can be derived from eq 1:

$$A = \frac{J_w}{\Delta P - \Delta \pi_m} \tag{7}$$

Therefore, compared with water flux J_w, water permeability A (including both A_{np} and A_p) can more effectively reflect the performance of the membrane because it unifies the water flux without the influence of feed side concentration or applied pressure.

3. PORE STRUCTURE AND CORRESPONDING WATER DESALINATION PERFORMANCE

Carbon-based membranes have been extensively studied by a number of researchers,[3,27−29] and RO membranes have exhibited extraordinary performance in terms of permeability and selectivity. Also, enhanced fouling resistance and scalability to practical modules are also significant factors with regard to the evaluation of membrane materials. Carbon-based desalination membranes are commonly classified as carbon nanotubes (CNTs), nanoporous graphene (NPG), and graphene-based frameworks. On the contrary, according to the hydrodynamic mechanism, the membrane can be proposed to be a porous structure and a nonporous structure. Specifically, the porous structure can be classified as a horizontal pore (Figure 3A) and a hollow nanochannel (Figure 3B) on the active layer. The nonporous structure is also divided into the tent-shaped lateral channel (Figure 3C) and the quasi-uniform lateral channel (Figure 3D). The following sections discuss different RO membranes with different pore geometric structures and their corresponding advantages in terms of water desalination performance and limitations.

3.1. Horizontal Pore on an Active Layer. The general idea for water desalination is transporting water molecules from one side of a membrane to the other while rejecting the salinity. Herein, the simplest method is fabricating lateral pores on the surface of 2D materials. A single-atom-thick graphene layer with a precisely controlled pore size is an ideal separation membrane. Grossman et al.[43] simulated the molecular

https://dx.doi.org/10.1021/acsestwater.0c00015
ACS EST Water XXXX, XXX, XXX−XXX

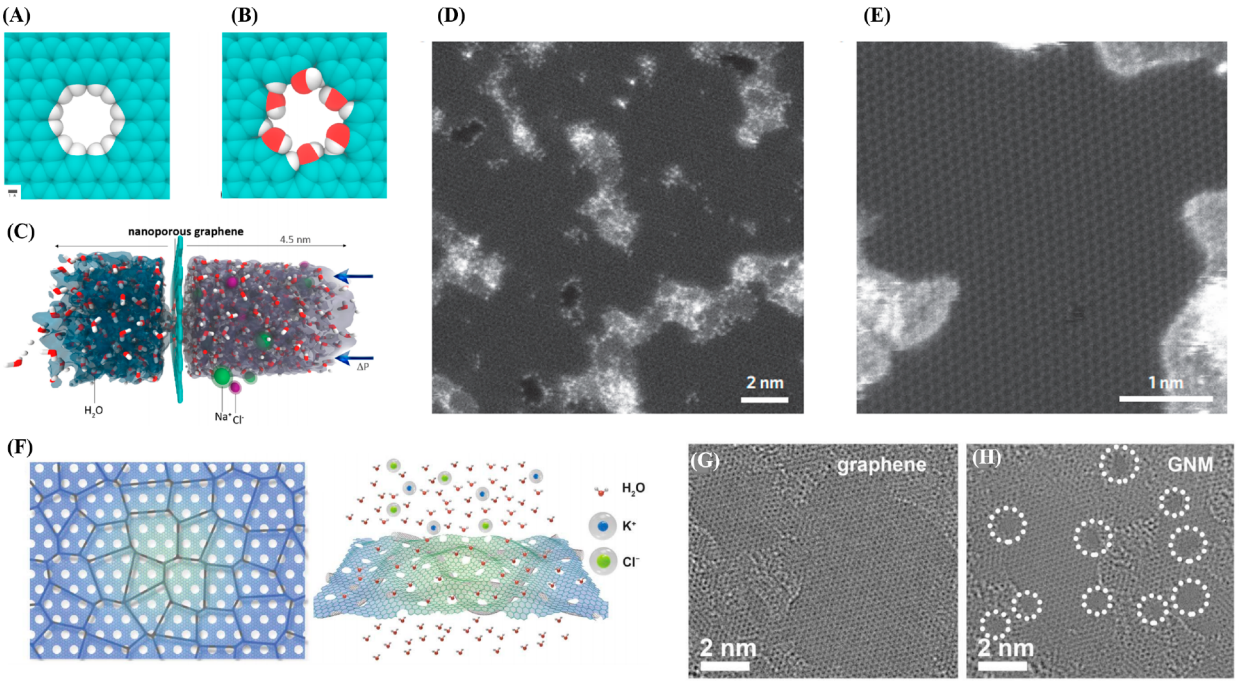

Figure 4. MD simulation model of (A) hydrogenated graphene pores, (B) hydroxylated graphene pores, and (C) the complete computational system. Reprinted with permission from ref 43. Copyright 2012 American Chemical Society). (D and E) Experimental scanning transmission electron microscope (STEM) images of graphene exposed to oxygen plasma. Reprinted with permission from ref 46. Copyright 2015 Springer Nature. (F–H) Schematic of the large-area GNM/SWNT hybrid membrane for efficient water desalination and corresponding experimental results. Reprinted with permission from ref 47. Copyright 2019 The American Association for the Advancement of Science.

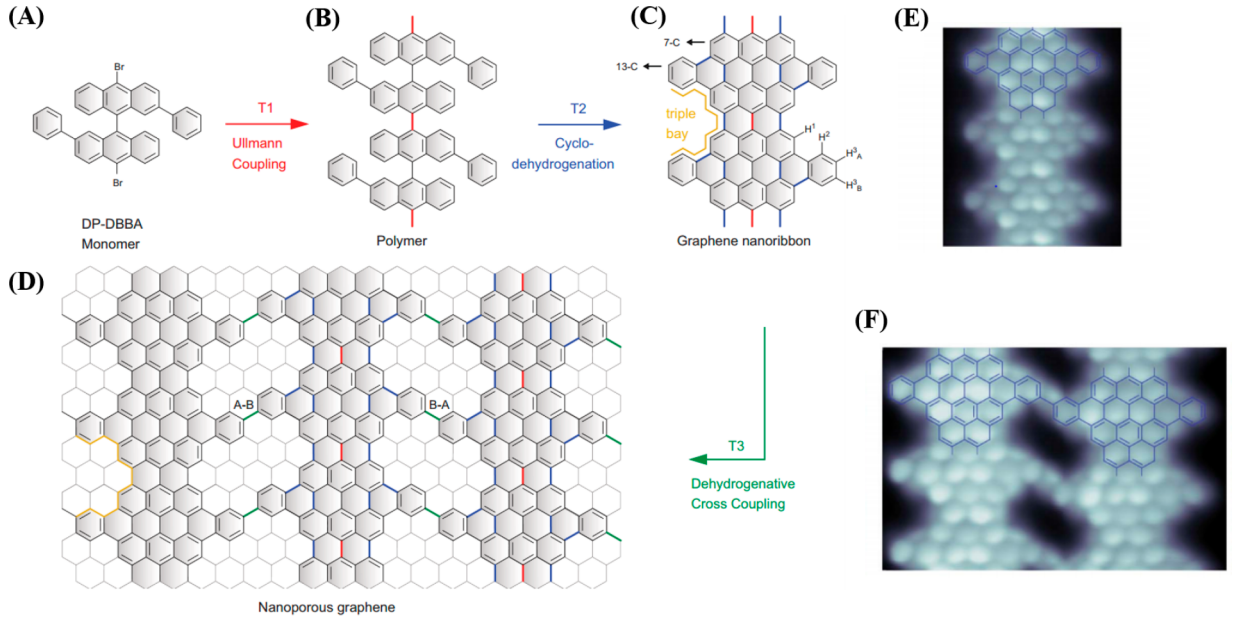

Figure 5. (A–D) Schematic illustration of the synthetic path for NPG and (E and F) corresponding illustrations of STM images. Reprinted with permission from ref 48. Copyright 2018 The American Association for the Advancement of Science.

dynamics through a single pore on single-layer graphene. In their model, a water molecule can pass through the pore while the salt ions are rejected with a largest pore size of 0.55 nm (as shown in Figure 4A–C). The water flux is also predicted to be several orders of magnitude higher than that of the existing RO membrane because of the extremely small thickness of the membrane. Other simulation attempts reported later provided a more comprehensive understanding of functionalized NPG membranes.[44,45] Besides the simulation results, such a single-layer NPG has been produced.[46] The author grew single-layer graphene via chemical vapor deposition (CVD) on a copper foil with the boundary of size at 50 μm, and then the single-layer nondefect graphene was transferred to a silicon nitride substrate with a 2 μm hole for the desalination test. To generate subnanometer pores on graphene, oxygen plasma etching is applied to single-layer graphene to remove carbon atoms from the 2D lattice. Via the precise control of exposure time and power, the pore size of the NPG is confined to the

https://dx.doi.org/10.1021/acsestwater.0c00015
ACS EST Water XXXX, XXX, XXX–XXX

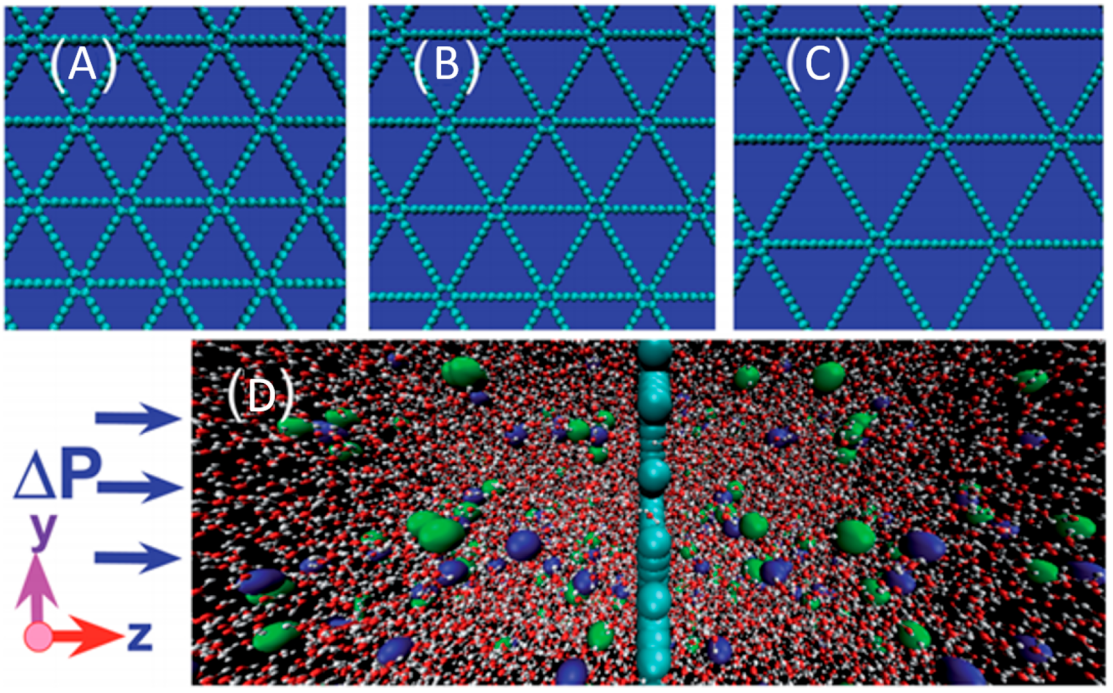

Figure 6. Three typical graphyne membranes: (A) graphyne-3, (B) graphyne-4, and (C) graphyne-5. (D) Snapshot of the simulation framework from ref 55. Reprinted with permission from ref 55. Copyright 2014 Royal Society of Chemistry.

range of 0.5−1 nm, which is the anticipated optimal pore size for ion sieving and water permeation, and the pore density is on the order of 1/100 nm^2. The ion rejection rate of the single-layer NPG is nearly 100%, exceeding those of most of the reported desalination membranes. The membrane also exhibited an outstanding water flux of $\leq 10^6$ g m^{-2} s^{-1} at 40 °C driven by a pressure difference, while the water flux driven by osmotic pressure is <70 g m^{-2} s^{-1} atm^{-1}. In 2019, Yang et al.[47] fabricated large-area graphene nanomesh (GNM) with the help of a single-walled carbon nanotube (SWNT) that acts as the mask during the plasma treatment process (as shown in Figure 4F−H). GNM/SWNT exhibited a value of 24 L m^{-2} h^{-1} bar^{-1}, which is 30 times larger than that of single-layer graphene with SWNT, and retained a salt rejection of ≤95.3% after osmotic operation for 24 h. The high water permeance and excellent ion selectivity make GNM/SWNT hybrid membranes highly attractive for energy-efficient and robust water treatment, but the cost of large-scale single-layer graphene may be the barrier for broadening this technique into industrial applications.

In addition to the top-down fabrication process, nanoporous graphene can also be synthesized via the bottom-up method.[48] The method consists of three thermally activated reaction steps with hierarchical control (as shown in Figure 5). Graphene nanoribbons (GNRs) are prepared first by surface-assisted Ullmann coupling of aromatic dihalide monomers into polymer chains. Then the cyclo-dehydrogenative aromatization of the intermediate polymeric chains was also grafted into GNRs. Next, the GNRs would be interconnected laterally in a reproducible manner employing a highly selective dehydrogenative cross-coupling, which requires a careful design of the monomer precursor. After deposition and annealing under the proper conditions, the C−C bond can be formatted. The resulting polymeric chains exhibit periodic nanopores that are 0.84 nm in diameter and 0.31 nm in height. Although the NPG prepared by the bottom-up method has not yet been applied to water desalination, it is still a significant breakthrough for NPG fabrication and desalination applications.

Although the water flux of NPG is several orders of magnitude higher than that of current RO membranes, it is still restricted in the laboratory because of the formation of large-scale single-layer defect-free graphene with a high density of porosity and pore size control is very challenging.[31] Besides NPG, graphyne, as a brother of graphene, also exhibits potential for water desalination. Displaying a uniform lattice of 2D sp−sp^2-hybridized carbon atoms, aromatic carbons of graphyne are bonded by single−triple−single carbon bonds[49] (shown in Figure 6A). Compared with other RO membranes, pristine graphyne and its derivatives exhibit an almost 100% rejection rate for nearly all ions in seawater, including Na^+, Cl^-, Mg^{2+}, K^+, and Ca^{2+}, at an exceptionally high water permeability that is ∼2 orders of magnitude higher than those for commercial state-of-the-art reverse osmosis membranes at a salt rejection of ∼98.5%.[50] This complete ion rejection rate is attributed to the significantly higher energy barriers for ions than for water molecules. The separation performance of this type of material is still at the stage of numerical simulation. Guo et al.[51] summarized the simulation results of different graphyne types with various methods, including molecular dynamics (MD) simulation,[50,52] quantum mechanics (QM) calculation,[53] and their combination.[54] Although there have been no experimental desalination achievements for this type of material, it provides a new possibility for the global water crisis and other environmental problems.

3.2. Hollow Nanochannels. Similar to horizontal pores, the hollow channels have the potential for remarkable performance for the water desalination process. With the proper choice of channel size, a water molecule can easily pass through while the salt ion will be rejected due to the steric effect. The first attempt to illustrate this strategy is by MD simulation. As early as 2001, the mechanism of water dynamics in single-walled (6, 6) carbon nanotubes (SWNT) had been

https://dx.doi.org/10.1021/acsestwater.0c00015
ACS EST Water XXXX, XXX, XXX−XXX

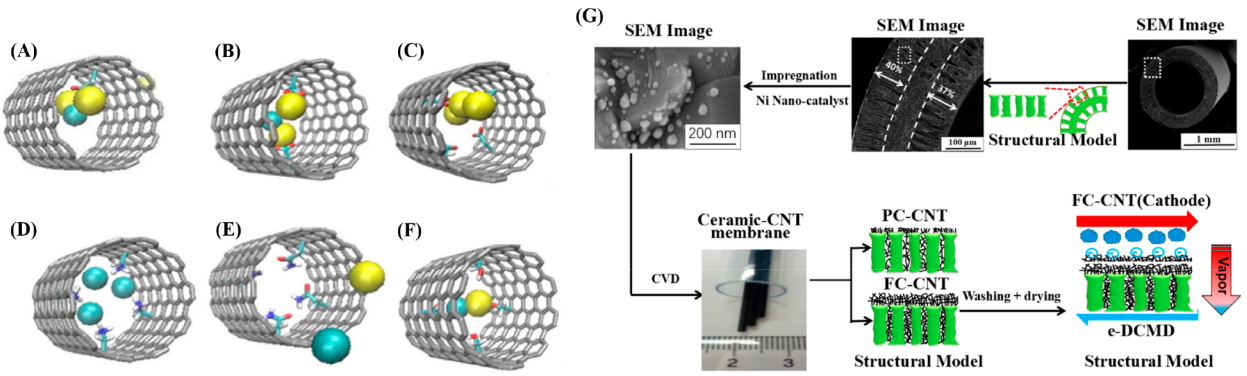

Figure 7. MD simulation of functionalized CNTs with (A) one COO^- group, (B) two COO^- groups, (C) four COO^- groups, (D) four NH_3^+ groups, (E) four $CONH_2$ groups, and (F) four OH groups. Reprinted with permission from ref 58. Copyright 2016 Elsevier. (G) Illustration of the fabrication and membrane desalination process of ceramic-based CNT membranes. Reprinted with permission from ref 59. Copyright 2018 American Chemical Society.

demonstrated.[56] Compared with NPG that exhibits extraordinary water flux because of the ultrathin thickness of the active membrane, SWNT also exhibits high water flux because of the atomically smooth, nonpolar interior forming a single-file water wire with ultrafast water conduction.[57] On the basis of the simulation results, the CNTs with a 0.81 nm center-to-center diameter and a 0.47 nm inner diameter have a 100% salt rejection rate while the (8, 8) CNTs with a 1.1 nm center-to-center diameter can exhibit an ion rejection rate of only 58%. Inspired by the structure of the biological membrane that has a perfect ion selectivity, polar and charged functional groups were grafted into the interior of CNTs (as shown in Figure 7A–F).[58] According to the MD simulation results, modified (10, 10) CNTs exhibit water flux that is 13 times higher that that of the traditional RO membrane. Meanwhile, modified CNTs with four COO^- or $CONH_2$ groups in the interior rejected 100% of the salt ions.

To achieve water desalination by hollow nanochannels, CNTs should be highly aligned to form a membrane. The earliest experimental fabrication of aligned CNTs was achieved by a CVD method.[60] Because the membrane consists of a multiwalled CNT that has a larger inner diameter, the average pore size of the membrane is around 1.6 nm. In this case, even if the water permeability of the membrane was 3–5 orders of magnitude higher than that calculated from continuum hydrodynamic models, the membrane can apply on only the UF instead of the NF due to the large pore size. Another bottom-up strategy for fabricating SWNTs also provides a new possible solution for aligned SWNTs.[61] The molecular precursors were converted into ultrashort singly capped (6, 6) "armchair" nanotube seeds using surface-catalyzed cyclodehydrogenation on a platinum (111) surface to produce single-chirality CNTs.

A more practical approach for hollow nanochannels is fabricating CNT-based composites.[59,62,63] Via application of a magnetic field and a template, the well-aligned SWNTs were sequestered in the micellar cores that formed hexagonally packed cylindrical liquid crystal mesophases.[63] Then the mesophase material was polymerized by ultraviolet treatment to form a polymer-based thin film embedded with vertically aligned SWNTs. More recently, researchers fabricated a superhydrophobic ceramic-based CNT membrane for membrane desalination (as shown in Figure 7G).[59] CNTs were grown in situ with quantitative regulation followed by the generation of a superporous and superhydrophobic surface structure. Although the membrane was tested under electrochemically assisted direct contact membrane desalination, the rejection rate of Na^+ is still as high as 99.9%.

For all hollow nanochannels, the critical issue is fabricating aligned SWNTs for the desalination process. Another challenge is compacting the aligned SWNTs as much as possible to achieve a large effective area for a high water permeability. Furthermore, scaling up is always an important technical concern for membrane fabrication that is well suited for desalination.

Another branch of the hollow structure for water desalination can be achieved with amorphous carbon. Fathy et al. used an amorphous carbon thin film (ACTF) to adsorb sodium ions from an aqueous solution.[64] The adsorption process of sodium ion was described by the linearized forms of Langmuir and Freundlich isotherm models. Compared with RO desalination based on the separation process, the energy consumption requirement in the adsorption process is very small. However, the lifetime and cost-effective rate for the adsorption process are quite small. Therefore, this method is not emphasized here.

3.3. Tent-Shaped Lateral Nanochannel. According to the theoretical calculation in section 2, effective water pathway length L is the critical factor of water permeability A. Compared with porous membranes in which water flows directly through the membrane, nonporous membranes require that the water molecule walk along the channels that are perpendicular to the direction of water flow. The water pathway of nonporous membranes is determined by the lateral size of the 2D materials, the thickness of the membranes, and the interlayer spacing between 2D material layers.[65] It is hard to evaluate whether a porous or a nonporous membrane is better, but we can still find some highlights for nonporous membranes that do not exist for porous structures. The transportation of ions through ultimately narrow slits can be ascribed to the little surface charge, which allows elucidation of the role of steric effects. According to the research of Geim et al., ions with hydrated diameters larger than the slit size can still permeate through, albeit with reduced mobility.[66] The mechanisms for the transport of water through graphene-based materials are expressed as membranes composed of GO laminates, which could be regarded as an assembly of many tiny carbon nanotubes stacked together with attached functional groups as spacers.[67]

https://dx.doi.org/10.1021/acsestwater.0c00015
ACS EST Water XXXX, XXX, XXX–XXX

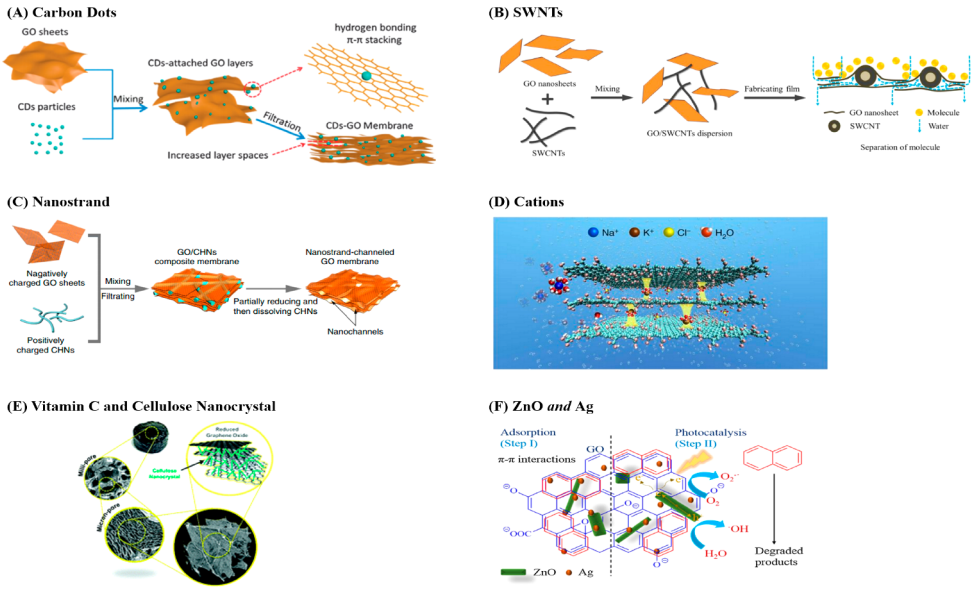

Figure 8. Schematic illustration of the tent-shaped channel of a GO membrane with different intercalations: (A) carbon dots (reprinted with permission from ref 74, copyright 2014 Royal Society of Chemistry), (B) SWNTs (reprinted with permission from ref 76, copyright 2014 Royal Society of Chemistry), (C) copper hydroxide nanostrand (reprinted with permission from ref 77, copyright 2013 Springer Nature), (D) cations (reprinted with permission from ref 78, copyright 2017 Springer Nature), (E) vitamin C and cellulose nanocrystal (CNC) (reprinted with permission from ref 79, copyright 2018 Royal Society of Chemistry), and (F) ZnO and Ag nanoparticles (reprinted with permission from ref 80, copyright 2020 Elsevier).

Because of the atomically smooth surface and thin layer, graphene-based materials become natural candidates for water desalination. The mechanism of the nonporous graphene desalination process is shown in Figure 8. To achieve a sufficient ion selectivity for different concentrations of feed water, nonporous graphene should comprise a multilayer stack of finite-sized graphene sheets. Generally, graphene-based nonporous membranes were fabricated via vacuum filtration or layer-by-layer (LBL) assembly of graphene oxide (GO), which is commonly oxidized from graphite and exfoliated to a single layer.[68−71] Recalling the advantages of CNTs that possess an atomically smooth channel for water molecules moving without friction, we found the GO layer with a number of hydrophilic groups also exhibits the same benefits. Compared to previous NPG and hollow nanochannel structures, the lateral one has been extensively studied due to its simplicity. In 2014, a group of researchers from The University of Manchester first studied stacked graphene oxide layers for water desalination. To increase the selectivity, the interlayer spacing of GO laminates should be precisely controlled. They proved that after vacuum filtration, the formed GO laminates exhibited an interlayer spacing of 0.9 ± 0.1 nm in humid air while the interlayer spacing will significantly increase to 1.3 ± 0.1 nm in water, which cannot reject the monovalent or divalent cations or the corresponding counterions.[72] To improve the selectivity of the multilayer stacked GO membrane, Su et al. tried to decrease the interlayer spacing via the reduction of GO into reduced graphene oxide (rGO).[73] In this case, several strategies were used to tune the interlayer spacing to accomplish the goal of ion selectivity.

The first strategy is insertion of solid particles as intercalations to tune the interlayer spacing. In this situation, GO sheets were supported by the intercalation to form a tent-shaped nanochannel that allows water molecules to pass through. In the work conducted by Gao et al. (as shown in Figure 8A), GO laminates were embedded with carbon nanodots of controllable sizes to tune the interlayer spacing.[74] Because the actual size of carbon nanodots is in the range of 1−8 nm, the as-prepared membrane was not designed to desalinate but to separate dyes from water, which shows 99% dye removal efficiency. Similarly, MnO_2 nanodots have also been tested as intercalations.[75] The SWNT is another choice for intercalation (as shown in Figure 8B).[76] GO/SWNT dispersions with different weight ratios were prepared followed by diluting and vacuum filtration. The interlayer spacing was also too large to achieve water desalination even if the water flux is 10-fold higher than those of traditional NF membranes. Compared to the intercalation remaining inside the membrane, dissolving the intercalation can significantly increase the water flux.[77] By inserting and dissolving as-prepared 3−5 nm carbon hydroxide nanostrands in GO frameworks, one finds the membrane exhibits 100-fold higher water permeance compared with those of commercial UF membranes. Although the membrane is not proper for NF and RO desalination, the strategy of intercalation removal is still inspiring. An outstanding breakthrough in this method to achieve water desalination was presented by Chen et al. in 2017.[78] They enlarged the interlayer spacing of graphene oxide sheets by inserting cations such as K^+, Na^+, Ca^{2+}, Li^+, and Mg^{2+}. The interlayer spacing can be fixed at 1.15 nm using KCl, which can steadily reject 99% of the Na^+ during water desalination for a long period of time. Although the water permeability of this membrane is only ∼0.36 L m^{-2} h^{-1} bar^{-1}, it still provides a new vision for a GO-based membrane for water desalination, which brings the GO framework membranes from the UF and NF range to RO membranes. In addition to water desalination, this method was also applied to achieve wastewater treatment, which focuses on larger particles compared to the salt ions in salinity. A vitamin C and cellulose nanocrystal (CNC) was used as an insertion to fabricate GO-based sponges for adsorption of water contaminants.[79] Another group fabricated a GO/ZnO/Ag nanocomposite to remove naphthalene from

https://dx.doi.org/10.1021/acsestwater.0c00015
ACS EST Water XXXX, XXX, XXX−XXX

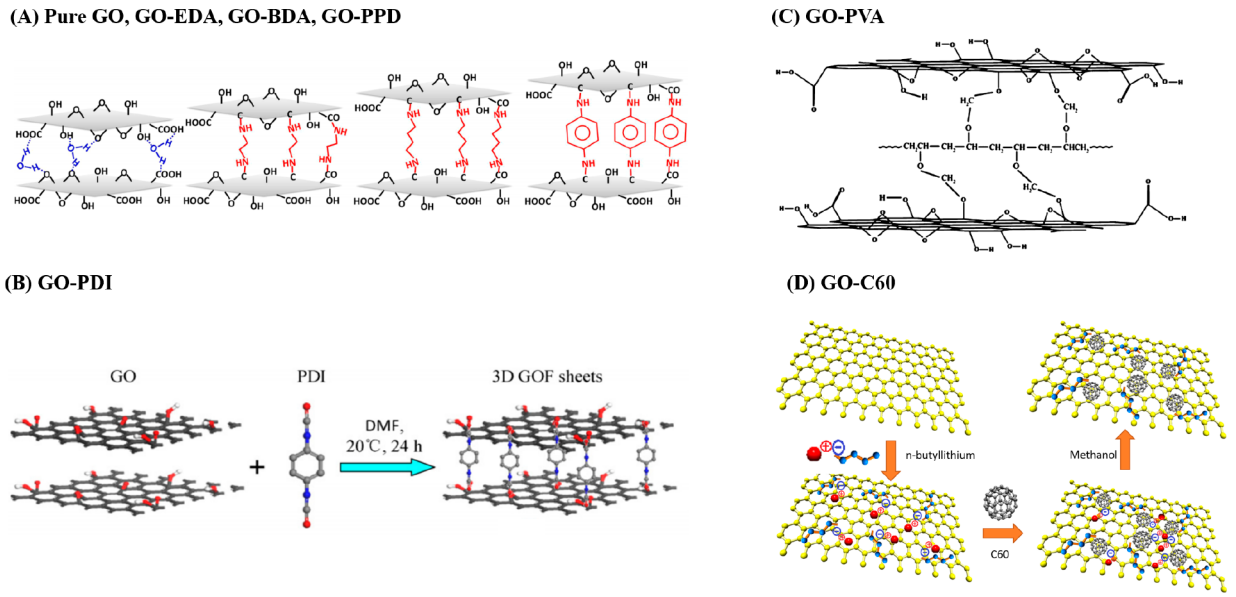

Figure 9. Schematic illustration of the quasi-uniform lateral channel of the GO membrane with different cross-linkers (A) EDA, BDA, and PPD (reprinted with permission from ref 84, copyright 2014 American Chemical Society), (B) PDI (reprinted with permission from ref 86, copyright 2016 Elsevier), (C) PVA (reprinted with permission from ref 87, copyright 2018 American Chemical Society), and (D) C60 (reprinted with permission from ref 88, copyright 2018 American Chemical Society).

wastewater through adsorption and photodegradation.[80] These approaches used a GO-based structure to achieve water purification by an adsorption process, which is not the focus of this review. Therefore, we will not elaborate on the specific discussion of this topic.

Because the tent-shaped structure inserts intercalations into GO sheets, the interlayer spacing is not uniform. The membranes also might swell in water surroundings. An unfixed and non-uniform interlayer spacing will reduce both the ion selectivity and the water permeability.

3.4. Quasi-uniform Lateral Nanochannel. Pure GO laminates possess natural ∼0.7−1.1 nm nanocapillary channels.[81] Compared with a tent-shaped lateral nanochannel, tuning and fixing the current GO interlayer spacing without inserting any intercalation is another of the strategies.

Quasi-uniform channels, which means the interlayer spacing is nearly even, can effectively reject the salt ions. Geim et al. enlarged the interlayer spacing of GO laminates to ∼1 nm by varying the humidity of the environment.[82] The ingenious innovation of this research was used in the cross-sectional area for water desalination where the membrane was encapsulated by epoxy so that the water flux can be as high as 5 L m^{-2} h^{-1}.

Another bracket, consisting of covalent cross-linking, was used as intercalating materials to enlarge the interlayer spacing of GO.[83] The covalent bond, which is much stronger than the van der Waals force or hydrogen bond, provides more rigid interlayer spacing than solid intercalation to form quasi-uniform channels for water desalination. In an approach conducted by Hung et al.,[84] the interlayer spacing of GO laminates was tuned by cross-linking with diamine monomers. By grafting different monomers of various molecular lengths [such as ethylenediamine (EDA), butylenediamine (BDA), and *p*-phenylenediamine (PPD)], one can achieve an interlayer spacing between 0.87 and 1.04 nm in the dry state. Cross-linked membranes also exhibit good rigidity of the *d* spacing in the wet state. Using the same strategy of cross-linking, the GO-EDA membrane shows a high water permeability of 5.01 L m^{-2} h^{-1} bar^{-1} and an ∼40% rejection rate for NaCl.[85] PDI (1,4-phenylene diisocyanate) is another cross-linker.[86] By modification of the Al_2O_3 tube with PDI, the membrane can be fabricated on the surface of the Al_2O_3 tube by vacuum filtration. In this case, the membrane can be used as a load of the cross-flow unit for the desalination test while other membranes are tested on only the death-end unit. This design indicates that the GO framework with quasi-uniform lateral channels has great potential for scaling up. In 2018, Li et al.[87] used poly(vinyl alcohol) (PVA) as a separator for GO laminates for wastewater treatment. Due to their large interlayer spacing, this approach can be applied to adsorb only large particles [they used methylene blue (MB) in the literature] instead of salinity desalination.

In addition to diamine monomers, C60 is also selected as a kind of cross-linker for tuning the interlayer spacing.[88] C60 possesses the proper molecular length (0.7 nm) and rigidity, which allows it as a cross-linker to provide both high efficiency and stability. The literature also applied the cross-sectional method as mentioned in ref 82 and provided a water flux as high as 10.85 L m^{-2} h^{-1} bar^{-1} with an 89.66% NaCl rejection rate.

Compared with other strategies, cross-linked GO membranes with quasi-uniform lateral channels exhibit more potential for better water desalination performance due to their fixed interlayer spacing. Energy consumption and scalability are still significant challenges that should be addressed (Figure 9).

4. OUTLOOK

Future RO membranes for water desalination should achieve both high water permeability and high ion selectivity. To achieve this goal, the thinner active layer for ion sieving must exhibit better performance. Herein, carbon-based materials, especially graphene-based material that is only 0.335 nm thick with high stability, provide a broad prospect for next-generation membranes. Regardless of what structure is

https://dx.doi.org/10.1021/acsestwater.0c00015
ACS EST Water XXXX, XXX, XXX−XXX

Table 1. Summary of Carbon-Based Membrane Performance and Corresponding Test Conditiond

membrane	scalability	classification	concentration of the feed side (mol/L)	Pressure (bar)	water flux (L m^{-2} h^{-1})	rejection rate (%)	ref
GNM/SWNT	yes	GO framework	0.5	5	120	95.3	47
CNT/PMMA	yes	CNT	0.034	10.00	0.36	40.00	93
CNT-PA	yes	CNT	0.034	15.50	47.00	97.00	94
KCl-controlled GO (280 nm)	yes	GO framework	0.25	20.00	0.36	94.67	78
GO-PA (0.015 wt %)	yes	GO framework	0.034	20.50	59.40	93.80	95
PEI/GO (1 bar)	yes	GO framework	0.00862	1.00	6.10	42.00	96
GO-PA	yes	GO framework	0.034	15.50	16.28	99.00	97
GO-PA(LBL)	yes	GO framework	0.034	15.50	13.95	96.40	98
GO-NHS/EDC/ED/PA	yes	GO framework	0.05	27.60	40.02	97.80	99
GO-PA	yes	GO framework	0.034	15.00	29.58	97.00	100
rGO/TiO_2	yes	GO framework	0.034	15.00	51.30	99.45	101
PA/SMWNT	yes	TFC	0.034	16.00	23.61	90.00	102
zwitterion-CNT	no	CNT	0.034	24.10	25.00	98.00	103
NH_2-MWCNT	no	CNT	0.034	15.00	58.00	96.00	104
oxidized MWCNT	no	CNT	0.034	15.00	28.90	97.40	105
GO in 84% relative humidity	no	GO framework	0.1	15.00	4.50	97.78	82
SWNT/TNT	no	TFC	0.034	15.00	11.10	97.97	106

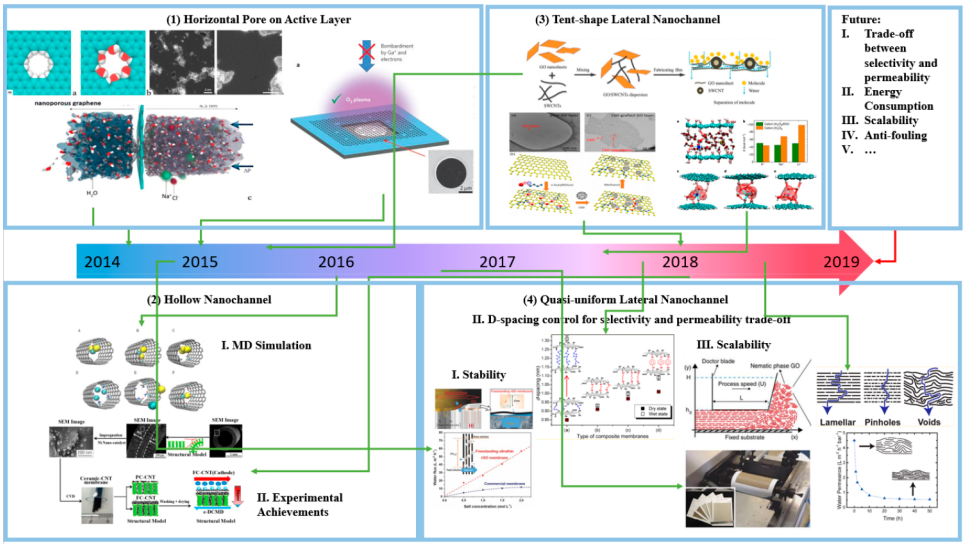

Figure 10. Evolution of carbon-based RO membranes and the prospect of future work. Adapted with permission from ref 43 (copyright 2012 American Chemical Society), ref 46 (copyright 2015 Springer Nature), ref 58 (copyright 2016 Elsevier), ref 59 (copyright 2018 American Chemical Society), ref 76 (copyright 2014 Royal Society of Chemistry), ref 78 (copyright 2017 Springer Nature), ref 84 (copyright 2014 American Chemical Society), ref 65 (copyright 2018 American Chemical Society), ref 90 (copyright 2015 John Wiley and Sons), and ref 91 (copyright 2016 Springer Nature).

designed, the general idea is achieving a high-selectivity and -permeability filter by allowing the molecules that are smaller than the pores to pass through. We have summarized the desalination performance of carbon-based materials as RO membranes that have been studied in the past five years (as shown in Table 1). To evaluate the RO desalination performance, the ion concentration of the feed side and the applied pressure that is related to the osmotic pressure, and the corresponding net pressure ($\Delta P - \Delta\pi$), are also important. Considering only the water desalination performance, horizontal pores on the active layer and quasi-uniform lateral nanochannels have the broadest prospects in the area of RO desalination. The trade-off between ion selectivity and water permeability is easy to understand. However, according to the research by Werber et al.,[89] if the water permeance reaches 2–4 L m^{-2} h^{-1} bar^{-1}, which is twice that of current commercial membranes for SWRO, the efficiency improvement with an increase in water permeability can be very marginal. The key issue for SWRO and wastewater RO for potable reuse is a nearly perfect ion rejection rate at any ionic strength and very high rejection of small neutral species.

In addition to that, the scalability, antifouling property, and energy consumption are also important factors that drive the design of the new generation of RO membranes. Figure 10 shows the evolution of carbon-based RO membranes and the prospect of future work.

Scalability is the most significant issue that blocks the path of carbon-based materials from laboratory to industrialization. A high uniformity and a high density of a 1 nm pore size fabrication without complex and expensive processes in the industry are still challenging to achieve.

https://dx.doi.org/10.1021/acsestwater.0c00015
ACS EST Water XXXX, XXX, XXX−XXX

According to a previous review, the horizontal pores on the active layer exhibit the best RO desalination performance and present the most difficulty in scaling up. The lateral nanochannels between 2D material stacks are the most feasible strategy for achieving scalability by intercalating nanomaterials between the layers. Therefore, the combination of these two methods could be a promising strategy for addressing the scale-up problems,[92] which means that the water molecules can travel both through and around the membranes. Compared to single-layer nanoporous GO, several layers of nanoporous GO laminates are much easier to fabricate. Furthermore, the uniformity of the pore size for GO laminates is not as high as that of single-layer GO. On the contrary, the water permeability of this strategy can be higher than that of using lateral nanochannels only due to the horizontal pores on the active layer. However, the selection and preparation of intercalation materials still require delicate consideration to achieve scaling up. The density of nanopores on the active layer is another concern that can significantly influence the water permeability and ion selectivity.

Considering the implications of membrane surface chemistry on membrane fouling, hydrophilicity is the most significant issue. Hydrophobic membranes possess high permeability, but the sustainability in liquid with organics is very low. On the contrary, hydrophilic membranes normally exhibit less severe organic fouling. Also, the high water flux will increase the concentration polarization, which in turn reduces the water flux. Conventionally, the strategies of RO membrane fouling mitigation are physical and chemical pretreatment for feed water, chemical modification of the membranes, and periodic cleaning. All of these strategies will significantly increase the cost of water desalination and reduce the benefits. Therefore, the antifouling surface is another research direction for carbon-based RO membranes.

It seems that the energy consumption issue is the same as water permeability. However, the specific energy consumption during the desalination process is coming from not only membrane filtration resistance, osmotic pressure, and concentration polarization but also friction losses and pump inefficiency. The lateral factor is related to the applied pressure. Currently, conventional treatment of surface water consumes 0.3 kWh/m^3 while brackish water desalination and seawater desalination cost 1.25 and 3.25 kWh/m^3, respectively, on average, which limits the further development of desalination.[10] Although the energy consumed by osmotic pressure cannot be reduced, it is still a long journey to reduce other factors on energy consumption such as membrane filtration resistance, concentration polarization, and pump inefficiency.

Carbon-based materials have great potential for the next generation of RO desalination membranes. However, the commercialization for such membranes still requires much work. For the short term, pore structure design for molecular selectivity, chemical properties for antifouling, membrane structure for water flux, and scalability should be addressed one by one to achieve extraordinary RO desalination performance. The long-term goals will be to design new desalination plants to accommodate the new generation of carbon-based RO membranes.

AUTHOR INFORMATION

Corresponding Author

Shiren Wang − *Department of Industrial and Systems Engineering and Department of Materials Science and Engineering, Texas A&M University, College Station, Texas 77843, United States;* orcid.org/0000-0003-4516-3025; Email: s.wang@tamu.edu

Authors

Yuchen Liu − *Department of Industrial and Systems Engineering, Texas A&M University, College Station, Texas 77843, United States;* orcid.org/0000-0002-3815-7818

Zimeng Zhang − *Department of Industrial and Systems Engineering, Texas A&M University, College Station, Texas 77843, United States*

Complete contact information is available at: https://pubs.acs.org/10.1021/acsestwater.0c00015

Author Contributions

S.W. conceived the research. Y.L., Z.Z., and S.W. wrote the manuscript. All authors have given approval to the final version of the manuscript.

Notes

The authors declare no competing financial interest.

ACKNOWLEDGMENTS

The authors appreciate the support of a Water Initiative Grant from Texas A&M AgriLife and the State of Texas and National Science Foundation Grants CMMI-1934120 and CMMI-1933679.

REFERENCES

(1) AQUASTAT Food and Agriculture Organization of the United Nations (FAO). AQUASTAT - FAO's Global Information System on Water and Agriculture. http://www.fao.org/nr/water/aquastat/water_use/index.stm (accessed 2019-10-01).

(2) Sapkota, A. R. *Water reuse, food production and public health: Adopting transdisciplinary, systems-based approaches to achieve water and food security in a changing climate*; Elsevier, 2019.

(3) Teow, Y. H.; Mohammad, A. W. New generation nanomaterials for water desalination: A review. *Desalination* **2019**, *451*, 2−17.

(4) U.S. Geological Survey. How Much Water is There on Earth? https://water.usgs.gov/edu/earthhowmuch.html (accessed 2019-10-01).

(5) Rodell, M.; Famiglietti, J.; Wiese, D.; Reager, J.; Beaudoing, H.; Landerer, F.; Lo, M.-H. Emerging trends in global freshwater availability. *Nature* **2018**, *557* (7707), 651.

(6) Shenvi, S. S.; Isloor, A. M.; Ismail, A. A review on RO membrane technology: developments and challenges. *Desalination* **2015**, *368*, 10−26.

(7) Elimelech, M.; Phillip, W. A. The future of seawater desalination: energy, technology, and the environment. *Science* **2011**, *333* (6043), 712−717.

(8) García-Pacheco, R.; Landaburu-Aguirre, J.; Terrero-Rodríguez, P.; Campos, E.; Molina-Serrano, F.; Rabadán, J.; Zarzo, D.; García-Calvo, E. Validation of recycled membranes for treating brackish water at pilot scale. *Desalination* **2018**, *433*, 199−208.

(9) Liu, Q.; Xu, G.-R. Graphene oxide (GO) as functional material in tailoring polyamide thin film composite (PA-TFC) reverse osmosis (RO) membranes. *Desalination* **2016**, *394*, 162−175.

(10) Voutchkov, N. Energy use for membrane seawater desalination−current status and trends. *Desalination* **2018**, *431*, 2−14.

(11) Werber, J. R.; Osuji, C. O.; Elimelech, M. Materials for next-generation desalination and water purification membranes. *Nat. Rev. Mater.* **2016**, *1* (5), 16018.

(12) Humplik, T.; Lee, J.; O'hern, S.; Fellman, B.; Baig, M.; Hassan, S.; Atieh, M.; Rahman, F.; Laoui, T.; Karnik, R.; Wang, E. N. Nanostructured materials for water desalination. *Nanotechnology* **2011**, *22* (29), 292001.
(13) Zhao, F.-Y.; Ji, Y.-L.; Weng, X.-D.; Mi, Y.-F.; Ye, C.-C.; An, Q.-F.; Gao, C.-J. High-flux positively charged nanocomposite nanofiltration membranes filled with poly (dopamine) modified multiwall carbon nanotubes. *ACS Appl. Mater. Interfaces* **2016**, *8* (10), 6693−6700.
(14) Zhang, C.; Wei, K.; Zhang, W.; Bai, Y.; Sun, Y.; Gu, J. Graphene oxide quantum dots incorporated into a thin film nanocomposite membrane with high flux and antifouling properties for low-pressure nanofiltration. *ACS Appl. Mater. Interfaces* **2017**, *9* (12), 11082−11094.
(15) Song, X.; Zambare, R. S.; Qi, S.; Sowrirajalu, B. N.; James Selvaraj, A. P.; Tang, C. Y.; Gao, C. Charge-Gated Ion Transport through Polyelectrolyte Intercalated Amine Reduced Graphene Oxide Membranes. *ACS Appl. Mater. Interfaces* **2017**, *9* (47), 41482−41495.
(16) Chen, B.; Jiang, H.; Liu, X.; Hu, X. Molecular insight into water desalination across multilayer graphene oxide membranes. *ACS Appl. Mater. Interfaces* **2017**, *9* (27), 22826−22836.
(17) Tang, C.; Wang, Z.; Petrinić, I.; Fane, A. G.; Hélix-Nielsen, C. Biomimetic aquaporin membranes coming of age. *Desalination* **2015**, *368*, 89−105.
(18) Sun, L.; Huang, H.; Peng, X. Laminar MoS 2 membranes for molecule separation. *Chem. Commun.* **2013**, *49* (91), 10718−10720.
(19) Lau, W.; Ismail, A.; Misdan, N.; Kassim, M. A recent progress in thin film composite membrane: a review. *Desalination* **2012**, *287*, 190−199.
(20) Feng, J.; Graf, M.; Liu, K.; Ovchinnikov, D.; Dumcenco, D.; Heiranian, M.; Nandigana, V.; Aluru, N. R.; Kis, A.; Radenovic, A. Single-layer MoS 2 nanopores as nanopower generators. *Nature* **2016**, *536* (7615), 197−200.
(21) Ntakadzeni, M.; Anku, W. W.; Kumar, N.; Govender, P. P.; Reddy, L. PEGylated MoS2 Nanosheets: A Dual Functional Photocatalyst for Photodegradation of Organic Dyes and Photoreduction of Chromium from Aqueous Solution. *Bull. Chem. React. Eng. Catal.* **2019**, *14* (1), 142−152.
(22) Kim, H. W.; Yoon, H. W.; Yoon, S.-M.; Yoo, B. M.; Ahn, B. K.; Cho, Y. H.; Shin, H. J.; Yang, H.; Paik, U.; Kwon, S.; Choi, J.Y.; Park, H. B. Selective gas transport through few-layered graphene and graphene oxide membranes. *Science* **2013**, *342* (6154), 91−95.
(23) Koenig, S. P.; Wang, L.; Pellegrino, J.; Bunch, J. S. Selective molecular sieving through porous graphene. *Nat. Nanotechnol.* **2012**, *7* (11), 728.
(24) Li, H.; Song, Z.; Zhang, X.; Huang, Y.; Li, S.; Mao, Y.; Ploehn, H. J.; Bao, Y.; Yu, M. Ultrathin, molecular-sieving graphene oxide membranes for selective hydrogen separation. *Science* **2013**, *342* (6154), 95−98.
(25) Wang, H.; Yang, Y.; Liang, Y.; Robinson, J. T.; Li, Y.; Jackson, A.; Cui, Y.; Dai, H. Graphene-wrapped sulfur particles as a rechargeable lithium−sulfur battery cathode material with high capacity and cycling stability. *Nano Lett.* **2011**, *11* (7), 2644−2647.
(26) Yao, F.; Gunes, F.; Ta, H. Q.; Lee, S. M.; Chae, S. J.; Sheem, K. Y.; Cojocaru, C. S.; Xie, S. S.; Lee, Y. H. Diffusion mechanism of lithium ion through basal plane of layered graphene. *J. Am. Chem. Soc.* **2012**, *134* (20), 8646−8654.
(27) Yang, Z.; Ma, X.-H.; Tang, C. Y. Recent development of novel membranes for desalination. *Desalination* **2018**, *434*, 37−59.
(28) Goh, P.; Ismail, A.; Ng, B. Carbon nanotubes for desalination: performance evaluation and current hurdles. *Desalination* **2013**, *308*, 2−14.
(29) Cohen-Tanugi, D.; Grossman, J. C. Nanoporous graphene as a reverse osmosis membrane: recent insights from theory and simulation. *Desalination* **2015**, *366*, 59−70.
(30) Qasim, M.; Badrelzaman, M.; Darwish, N. N.; Darwish, N. A.; Hilal, N. Reverse osmosis desalination: A state-of-the-art review. *Desalination* **2019**, *459*, 59−104.
(31) Boretti, A.; Al-Zubaidy, S.; Vaclavikova, M.; Al-Abri, M.; Castelletto, S.; Mikhalovsky, S. Outlook for graphene-based desalination membranes. *npj Clean Water* **2018**, *1* (1), 5.
(32) Gusain, R.; Kumar, N.; Ray, S. S. Recent advances in carbon nanomaterial-based adsorbents for water purification. *Coord. Chem. Rev.* **2020**, *405*, 213111.
(33) Saleem, H.; Zaidi, S. J. Nanoparticles in reverse osmosis membranes for desalination: A state of the art review. *Desalination* **2020**, *475*, 114171.
(34) Yang, Z.; Zhou, Y.; Feng, Z.; Rui, X.; Zhang, T.; Zhang, Z. A review on reverse osmosis and nanofiltration membranes for water purification. *Polymers* **2019**, *11* (8), 1252.
(35) Pakulski, D.; Czepa, W.; Buffa, S. D.; Ciesielski, A.; Samorì, P. Atom-thick membranes for water purification and blue energy harvesting. *Adv. Funct. Mater.* **2020**, *30* (2), 1902394.
(36) Yang, K.; Wang, J.; Chen, X.; Zhao, Q.; Ghaffar, A.; Chen, B. Application of graphene-based materials in water purification: from the nanoscale to specific devices. *Environ. Sci.: Nano* **2018**, *5* (6), 1264−1297.
(37) Danda, G.; Drndić, M. Two-dimensional nanopores and nanoporous membranes for ion and molecule transport. *Curr. Opin. Biotechnol.* **2019**, *55*, 124−133.
(38) Xiong, H.; Yan, H. Simulating the infected population and spread trend of 2019-nCov under different policy by EIR model. *medRxiv* **2020**, DOI: 10.1101/2020.02.10.20021519.
(39) Xu, G.-R.; Xu, J.-M.; Su, H.-C.; Liu, X.-Y.; Lu-Li; Zhao, H.-L.; Feng, H.-J.; Das, R. Two-dimensional (2D) nanoporous membranes with sub-nanopores in reverse osmosis desalination: Latest developments and future directions. *Desalination* **2019**, *451*, 18−34.
(40) Mehta, A.; Zydney, A. L. Permeability and selectivity analysis for ultrafiltration membranes. *J. Membr. Sci.* **2005**, *249* (1-2), 245−249.
(41) Baker, R. W. *Membrane technology and applications*; John Wiley & Sons, 2012.
(42) Geise, G. M.; Paul, D. R.; Freeman, B. D. Fundamental water and salt transport properties of polymeric materials. *Prog. Polym. Sci.* **2014**, *39* (1), 1−42.
(43) Cohen-Tanugi, D.; Grossman, J. C. Water desalination across nanoporous graphene. *Nano Lett.* **2012**, *12* (7), 3602−3608.
(44) Hosseini, M.; Azamat, J.; Erfan-Niya, H. Improving the performance of water desalination through ultra-permeable functionalized nanoporous graphene oxide membrane. *Appl. Surf. Sci.* **2018**, *427*, 1000−1008.
(45) Hosseini, M.; Azamat, J.; Erfan-Niya, H. Water desalination through fluorine-functionalized nanoporous graphene oxide membranes. *Mater. Chem. Phys.* **2019**, *223*, 277−286.
(46) Surwade, S. P.; Smirnov, S. N.; Vlassiouk, I. V.; Unocic, R. R.; Veith, G. M.; Dai, S.; Mahurin, S. M. Water desalination using nanoporous single-layer graphene. *Nat. Nanotechnol.* **2015**, *10* (5), 459.
(47) Yang, Y.; Yang, X.; Liang, L.; Gao, Y.; Cheng, H.; Li, X.; Zou, M.; Ma, R.; Yuan, Q.; Duan, X. Large-area graphene-nanomesh/carbon-nanotube hybrid membranes for ionic and molecular nanofiltration. *Science* **2019**, *364* (6445), 1057−1062.
(48) Moreno, C.; Vilas-Varela, M.; Kretz, B.; Garcia-Lekue, A.; Costache, M. V.; Paradinas, M.; Panighel, M.; Ceballos, G.; Valenzuela, S. O.; Peña, D.; Mugarza, A. Bottom-up synthesis of multifunctional nanoporous graphene. *Science* **2018**, *360* (6385), 199−203.
(49) Cranford, S. W.; Buehler, M. J. Mechanical properties of graphyne. *Carbon* **2011**, *49* (13), 4111−4121.
(50) Xue, M.; Qiu, H.; Guo, W. Exceptionally fast water desalination at complete salt rejection by pristine graphyne monolayers. *Nanotechnology* **2013**, *24* (50), 505720.
(51) Qiu, H.; Xue, M.; Shen, C.; Zhang, Z.; Guo, W. Graphynes for water desalination and gas separation. *Adv. Mater.* **2019**, *31* (42), 1803772.
(52) Raju, M.; Govindaraju, P. B.; van Duin, A. C.; Ihme, M. Atomistic and continuum scale modeling of functionalized graphyne

https://dx.doi.org/10.1021/acsestwater.0c00015
ACS EST Water XXXX, XXX, XXX−XXX

membranes for water desalination. *Nanoscale* **2018**, *10* (8), 3969−3980.
(53) Yang, J.; Xu, Z.; Yang, X. Multiscale molecular simulations on interfacial adsorption and permeation of nanoporous graphynes. *Phys. Chem. Chem. Phys.* **2017**, *19* (32), 21481−21489.
(54) Zhu, C.; Li, H.; Zeng, X. C.; Wang, E.; Meng, S. Quantized water transport: ideal desalination through graphyne-4 membrane. *Sci. Rep.* **2013**, *3*, 3163.
(55) Kou, J.; Zhou, X.; Lu, H.; Wu, F.; Fan, J. Graphyne as the membrane for water desalination. *Nanoscale* **2014**, *6* (3), 1865−1870.
(56) Hummer, G.; Rasaiah, J. C.; Noworyta, J. P. Water conduction through the hydrophobic channel of a carbon nanotube. *Nature* **2001**, *414* (6860), 188.
(57) Corry, B. Designing carbon nanotube membranes for efficient water desalination. *J. Phys. Chem. B* **2008**, *112* (5), 1427−1434.
(58) Li, Q.; Yang, D.; Shi, J.; Xu, X.; Yan, S.; Liu, Q. Biomimetic modification of large diameter carbon nanotubes and the desalination behavior of its reverse osmosis membrane. *Desalination* **2016**, *379*, 164−171.
(59) Dong, Y.; Ma, L.; Tang, C. Y.; Yang, F.; Quan, X.; Jassby, D.; Zaworotko, M. J.; Guiver, M. D. Stable superhydrophobic ceramic-based carbon nanotube composite desalination membranes. *Nano Lett.* **2018**, *18* (9), 5514−5521.
(60) Holt, J. K.; Park, H. G.; Wang, Y.; Stadermann, M.; Artyukhin, A. B.; Grigoropoulos, C. P.; Noy, A.; Bakajin, O. Fast mass transport through sub-2-nanometer carbon nanotubes. *Science* **2006**, *312* (5776), 1034−1037.
(61) Sanchez-Valencia, J. R.; Dienel, T.; Gröning, O.; Shorubalko, I.; Mueller, A.; Jansen, M.; Amsharov, K.; Ruffieux, P.; Fasel, R. Controlled synthesis of single-chirality carbon nanotubes. *Nature* **2014**, *512* (7512), 61.
(62) Hinds, B. J.; Chopra, N.; Rantell, T.; Andrews, R.; Gavalas, V.; Bachas, L. G. Aligned multiwalled carbon nanotube membranes. *Science* **2004**, *303* (5654), 62−65.
(63) Mauter, M. S.; Elimelech, M.; Osuji, C. O. Nanocomposites of vertically aligned single-walled carbon nanotubes by magnetic alignment and polymerization of a lyotropic precursor. *ACS Nano* **2010**, *4* (11), 6651−6658.
(64) Fathy, M.; Mousa, M. A.; Moghny, T. A.; Awadallah, A. E. Characterization and evaluation of amorphous carbon thin film (ACTF) for sodium ion adsorption. *Appl. Water Sci.* **2017**, *7* (8), 4427−4435.
(65) Saraswat, V.; Jacobberger, R. M.; Ostrander, J. S.; Hummell, C. L.; Way, A. J.; Wang, J.; Zanni, M. T.; Arnold, M. S. Invariance of water permeance through size-differentiated graphene oxide laminates. *ACS Nano* **2018**, *12* (8), 7855−7865.
(66) Esfandiar, A.; Radha, B.; Wang, F.; Yang, Q.; Hu, S.; Garaj, S.; Nair, R.; Geim, A.; Gopinadhan, K. Size effect in ion transport through angstrom-scale slits. *Science* **2017**, *358* (6362), 511−513.
(67) Deng, J.; You, Y.; Bustamante, H.; Sahajwalla, V.; Joshi, R. K. Mechanism of water transport in graphene oxide laminates. *Chemical science* **2017**, *8* (3), 1701−1704.
(68) Hummers, W. S., Jr; Offeman, R. E. Preparation of graphitic oxide. *J. Am. Chem. Soc.* **1958**, *80* (6), 1339−1339.
(69) Marcano, D. C.; Kosynkin, D. V.; Berlin, J. M.; Sinitskii, A.; Sun, Z.; Slesarev, A.; Alemany, L. B.; Lu, W.; Tour, J. M. Improved synthesis of graphene oxide. *ACS Nano* **2010**, *4* (8), 4806−4814.
(70) Stankovich, S.; Dikin, D. A.; Piner, R. D.; Kohlhaas, K. A.; Kleinhammes, A.; Jia, Y.; Wu, Y.; Nguyen, S. T.; Ruoff, R. S. Synthesis of graphene-based nanosheets via chemical reduction of exfoliated graphite oxide. *Carbon* **2007**, *45* (7), 1558−1565.
(71) Bourlinos, A. B.; Gournis, D.; Petridis, D.; Szabó, T.; Szeri, A.; Dékány, I. Graphite oxide: chemical reduction to graphite and surface modification with primary aliphatic amines and amino acids. *Langmuir* **2003**, *19* (15), 6050−6055.
(72) Joshi, R.; Carbone, P.; Wang, F. C.; Kravets, V. G.; Su, Y.; Grigorieva, I. V.; Wu, H.; Geim, A. K.; Nair, R. R. Precise and ultrafast molecular sieving through graphene oxide membranes. *Science* **2014**, *343* (6172), 752−754.
(73) Su, Y.; Kravets, V.; Wong, S.; Waters, J.; Geim, A.; Nair, R. Impermeable barrier films and protective coatings based on reduced graphene oxide. *Nat. Commun.* **2014**, *5*, 4843.
(74) Wang, W.; Eftekhari, E.; Zhu, G.; Zhang, X.; Yan, Z.; Li, Q. Graphene oxide membranes with tunable permeability due to embedded carbon dots. *Chem. Commun.* **2014**, *50* (86), 13089−13092.
(75) El-Deen, A. G.; Barakat, N. A.; Kim, H. Y. Graphene wrapped MnO2-nanostructures as effective and stable electrode materials for capacitive deionization desalination technology. *Desalination* **2014**, *344*, 289−298.
(76) Gao, S. J.; Qin, H.; Liu, P.; Jin, J. SWCNT-intercalated GO ultrathin films for ultrafast separation of molecules. *J. Mater. Chem. A* **2015**, *3* (12), 6649−6654.
(77) Huang, H.; Song, Z.; Wei, N.; Shi, L.; Mao, Y.; Ying, Y.; Sun, L.; Xu, Z.; Peng, X. Ultrafast viscous water flow through nanostrand-channelled graphene oxide membranes. *Nat. Commun.* **2013**, *4*, 2979.
(78) Chen, L.; Shi, G.; Shen, J.; Peng, B.; Zhang, B.; Wang, Y.; Bian, F.; Wang, J.; Li, D.; Qian, Z.; et al. Ion sieving in graphene oxide membranes via cationic control of interlayer spacing. *Nature* **2017**, *550* (7676), 380.
(79) Yousefi, N.; Wong, K. K.; Hosseinidoust, Z.; Sørensen, H. O.; Bruns, S.; Zheng, Y.; Tufenkji, N. Hierarchically porous, ultra-strong reduced graphene oxide-cellulose nanocrystal sponges for exceptional adsorption of water contaminants. *Nanoscale* **2018**, *10* (15), 7171−7184.
(80) Mukwevho, N.; Gusain, R.; Fosso-Kankeu, E.; Kumar, N.; Waanders, F.; Ray, S. S. Removal of naphthalene from simulated wastewater through adsorption-photodegradation by ZnO/Ag/GO nanocomposite. *J. Ind. Eng. Chem.* **2020**, *81*, 393−404.
(81) Nair, R.; Wu, H.; Jayaram, P.; Grigorieva, I.; Geim, A. Unimpeded permeation of water through helium-leak−tight graphene-based membranes. *Science* **2012**, *335* (6067), 442−444.
(82) Abraham, J.; Vasu, K. S.; Williams, C. D.; Gopinadhan, K.; Su, Y.; Cherian, C. T.; Dix, J.; Prestat, E.; Haigh, S. J.; Grigorieva, I. V.; et al. Tunable sieving of ions using graphene oxide membranes. *Nat. Nanotechnol.* **2017**, *12*, 546.
(83) Mi, B. Graphene oxide membranes for ionic and molecular sieving. *Science* **2014**, *343* (6172), 740−742.
(84) Hung, W.-S.; Tsou, C.-H.; De Guzman, M.; An, Q.-F.; Liu, Y.-L.; Zhang, Y.-M.; Hu, C.-C.; Lee, K.-R.; Lai, J.-Y. Cross-linking with diamine monomers to prepare composite graphene oxide-framework membranes with varying d-spacing. *Chem. Mater.* **2014**, *26* (9), 2983−2990.
(85) Zhang, Y.; Zhang, S.; Chung, T.-S. Nanometric graphene oxide framework membranes with enhanced heavy metal removal via nanofiltration. *Environ. Sci. Technol.* **2015**, *49* (16), 10235−10242.
(86) Feng, B.; Xu, K.; Huang, A. Covalent synthesis of three-dimensional graphene oxide framework (GOF) membrane for seawater desalination. *Desalination* **2016**, *394*, 123−130.
(87) Li, X.; Liu, T.; Wang, D.; Li, Q.; Liu, Z.; Li, N.; Zhang, Y.; Xiao, C.; Feng, X. Superlight adsorbent sponges based on graphene oxide cross-linked with poly (vinyl alcohol) for continuous flow adsorption. *ACS Appl. Mater. Interfaces* **2018**, *10* (25), 21672−21680.
(88) Liu, Y.; Phillips, B.; Li, W.; Zhang, Z.; Fang, L.; Qiu, J.; Wang, S. Fullerene-tailored graphene oxide interlayer spacing for energy-efficient water desalination. *ACS Applied Nano Materials* **2018**, *1* (11), 6168−6175.
(89) Werber, J. R.; Deshmukh, A.; Elimelech, M. The critical need for increased selectivity, not increased water permeability, for desalination membranes. *Environ. Sci. Technol. Lett.* **2016**, *3* (4), 112−120.
(90) Liu, H.; Wang, H.; Zhang, X. Facile fabrication of freestanding ultrathin reduced graphene oxide membranes for water purification. *Adv. Mater.* **2015**, *27* (2), 249−254.
(91) Akbari, A.; Sheath, P.; Martin, S. T.; Shinde, D. B.; Shaibani, M.; Banerjee, P. C.; Tkacz, R.; Bhattacharyya, D.; Majumder, M. Large-area graphene-based nanofiltration membranes by shear

https://dx.doi.org/10.1021/acsestwater.0c00015
ACS EST Water XXXX, XXX, XXX−XXX

alignment of discotic nematic liquid crystals of graphene oxide. *Nat. Commun.* **2016**, *7* (1), 10891.
(92) Mi, B. Scaling up nanoporous graphene membranes. *Science* **2019**, *364* (6445), 1033−1034.
(93) Shen, J. n.; Yu, C. c.; Ruan, H. m.; Gao, C. j.; Van der Bruggen, B. Preparation and characterization of thin-film nanocomposite membranes embedded with poly (methyl methacrylate) hydrophobic modified multiwalled carbon nanotubes by interfacial polymerization. *J. Membr. Sci.* **2013**, *442*, 18−26.
(94) Baek, Y.; Kim, H. J.; Kim, S.-H.; Lee, J.-C.; Yoon, J. Evaluation of carbon nanotube-polyamide thin-film nanocomposite reverse osmosis membrane: Surface properties, performance characteristics and fouling behavior. *J. Ind. Eng. Chem.* **2017**, *56*, 327−334.
(95) Yin, J.; Zhu, G.; Deng, B. Graphene oxide (GO) enhanced polyamide (PA) thin-film nanocomposite (TFN) membrane for water purification. *Desalination* **2016**, *379*, 93−101.
(96) Goh, K.; Setiawan, L.; Wei, L.; Si, R.; Fane, A. G.; Wang, R.; Chen, Y. Graphene oxide as effective selective barriers on a hollow fiber membrane for water treatment process. *J. Membr. Sci.* **2015**, *474*, 244−253.
(97) Chae, H.-R.; Lee, J.; Lee, C.-H.; Kim, I.-C.; Park, P.-K. Graphene oxide-embedded thin-film composite reverse osmosis membrane with high flux, anti-biofouling, and chlorine resistance. *J. Membr. Sci.* **2015**, *483*, 128−135.
(98) Choi, W.; Choi, J.; Bang, J.; Lee, J.-H. Layer-by-layer assembly of graphene oxide nanosheets on polyamide membranes for durable reverse-osmosis applications. *ACS Appl. Mater. Interfaces* **2013**, *5* (23), 12510−12519.
(99) Perreault, F. o.; Tousley, M. E.; Elimelech, M. Thin-film composite polyamide membranes functionalized with biocidal graphene oxide nanosheets. *Environ. Sci. Technol. Lett.* **2014**, *1* (1), 71−76.
(100) Ali, M. E.; Wang, L.; Wang, X.; Feng, X. Thin film composite membranes embedded with graphene oxide for water desalination. *Desalination* **2016**, *386*, 67−76.
(101) Safarpour, M.; Khataee, A.; Vatanpour, V. Thin film nanocomposite reverse osmosis membrane modified by reduced graphene oxide/TiO2 with improved desalination performance. *J. Membr. Sci.* **2015**, *489*, 43−54.
(102) Zhao, H.; Qiu, S.; Wu, L.; Zhang, L.; Chen, H.; Gao, C. Improving the performance of polyamide reverse osmosis membrane by incorporation of modified multi-walled carbon nanotubes. *J. Membr. Sci.* **2014**, *450*, 249−256.
(103) Chan, W.-F.; Marand, E.; Martin, S. M. Novel zwitterion functionalized carbon nanotube nanocomposite membranes for improved RO performance and surface anti-biofouling resistance. *J. Membr. Sci.* **2016**, *509*, 125−137.
(104) Vatanpour, V.; Safarpour, M.; Khataee, A.; Zarrabi, H.; Yekavalangi, M. E.; Kavian, M. A thin film nanocomposite reverse osmosis membrane containing amine-functionalized carbon nanotubes. *Sep. Purif. Technol.* **2017**, *184*, 135−143.
(105) Farahbakhsh, J.; Delnavaz, M.; Vatanpour, V. Investigation of raw and oxidized multiwalled carbon nanotubes in fabrication of reverse osmosis polyamide membranes for improvement in desalination and antifouling properties. *Desalination* **2017**, *410*, 1−9.
(106) Wan Azelee, I.; Goh, P.; Lau, W.; Ismail, A.; Rezaei-DashtArzhandi, M.; Wong, K.; Subramaniam, M. Enhanced desalination of polyamide thin film nanocomposite incorporated with acid treated multiwalled carbon nanotube-titania nanotube hybrid. *Desalination* **2017**, *409*, 163−170.

https://dx.doi.org/10.1021/acsestwater.0c00015
ACS EST Water XXXX, XXX, XXX−XXX